Proceedings of International Collaboration on Advanced Neutron Sources (ICANS-VII), 1983 September 13-16
Atomic Energy of Canada Limited, Report AECL-8488

FERTILE-TO-FISSILE CONVERSION AND FISSION MEASUREMENTS FOR THORIUM BOMBARDED BY 800-MeV PROTONS

J. S. Gilmore, G. J. Russell, H. Robinson, and R. E. Prael
Los Alamos National Laboratory
P.O. Box 1663
Los Alamos, New Mexico 87545, U.S.A.

Summary

Axial distributions of fertile-to-fissile conversion (^{232}Th to ^{233}U), four spallation products, and 34 fission products have been measured for a thick thorium target bombarded by 800-MeV protons. Uranium-233 production was determined by measuring the amount of ^{233}Pa produced, and the number of fissions was deduced from the fission product yield curves. The axial distributions were integrated to get the total conversions and fissions occurring in the target. Our preliminary experimental results are 1.25 ± 0.06 atoms of ^{233}Pa produced per incident proton, and 1.56 ± 0.25 fissions per incident proton. Corresponding calculated results are 1.267 ± 0.007 and 1.543 ± 0.006.

Introduction

The work reported here is part of the Fertile-to-Fissile Conversion (FERFICON) program at the Los Alamos National Laboratory.[1, 2, 3] The experiment was conducted at the Weapons Neutron Research Facility (WNR)[4] using the 800-MeV proton source of the Clinton P. Anderson Meson Physics Facility (LAMPF).[5] We have measured ^{233}U production, thorium fission, four spallation products, and 34 fission products in a thick thorium target irradiated with 800-MeV protons. We determine ^{233}U production by measuring the amount of ^{233}Pa formed, and deduce the number of fissions from fission product mass-yield curves. Our experimental approach has been described previously.[3] Briefly, we explicitly measure the axial distribution of products by sampling various planes perpendicular to the target axis; the radial integral for each plane is performed by combining sampling-foils from the plane. We integrate the measured axial distributions over the target to obtain the total number of each reaction.

This measurement is a "clean" integral experiment, and the data are relevant to spallation neutron source development, accelerator breeder technology, and validating computer codes used in these applications. We compare measured quantities with calculated predictions.

Calculational Approach

At Los Alamos, we have the following Monte Carlo codes integrated into a package for use in spallation physics computations: a) the Oak Ridge National Laboratory (ORNL) code HETC[6] for particle transport >20 MeV, and b) the Los Alamos code MCNP[7] for neutron and photon transport <20 MeV. The Los Alamos code HTAPE, written by Dick Prael, is used to analyze the Monte Carlo results. We have operational the latest ORNL HETC version which includes high-energy fission effects for $Z \geq 91$, and the Rutherford Appleton Laboratory (RAL) HETC version, as modified by Atchison,[8] which allows high-energy fission with essentially no restriction on Z. With MCNP, we do continuous-energy Monte Carlo using pointwise ENDF/B-V cross sections.

In our calculations, we do a precise mockup of target geometry, target canister, proton beam window, and air paths. We simulate the measured proton beam profile with eleven concentric ring-sources, and obtain the proton fraction in each ring from the measured distribution.

Experimental Setup and Procedures

We used a 19-rod clustered target having the physical characteristics given in Table I. The axial distributions of reaction products were determined from ninety 41.94-mm-diameter by 0.254 mm-thick thorium foils. Ten weighed-and-matched, four-gm foils were placed in each of seven planes perpendicular to the target axis within the target, and on the front and back target faces (see Fig. 1). Each plane contained one foil in the central rod and nine foils loaded symmetrically in three of the six target sectors. We chose this loading for mechanical reasons, and to minimize any effects from misalignment of the proton beam, which was focussed on the central rod.

After the target assembly was irradiated with 1.91 x 10^{16} protons, nine solutions were prepared for counting by dissolving the foils in nitric acid containing small amounts of hydrochloric and hydrofluoric acids. For each plane, representative sampling was accomplished by combining one half of the solution of the central foil with the solution of the remaining nine foils. Five ml (2.5%) of the final solution was used for Ge(Li) gamma assay. One additional sample was prepared utilizing 5% of the foil on the front face of the central rod.

To determine the number of protons striking the target, a 0.254-mm-thick Al monitor foil (sandwiched between two 0.0254-mm-thick Al guard foils to compensate for recoil loss) was placed ~60 cm in front of the target. The number of $^{27}Al(p,x)^{7}Be$, $^{27}Al(p,x)^{22}Na$, and $^{27}Al(p,3pn)^{24}Na$ reactions occurring in the monitor foil were used to determine the incident proton dose (see Table II). The center of the beam was known from the discoloration of a cellophane foil which covered the monitor foil packet, and the proton beam profile was measured by counting concentric rings cut from one of the guard foils. The measured proton beam profile is shown in Fig. 2. Ninety-seven percent of the protons were within the diameter of the central rod.

All dissolved thorium samples were counted using a Ge(Li) detector and associated pulse height analyzer which had been calibrated against a mixed radionuclide gamma-ray reference standard.* The gamma-ray spectra were analyzed by the GAMANAL computer program.[9] After the samples had been counted 15 times over a period of 40 days, the decay data were processed by the CLSQ program.[10] Strontium-89, ^{90}Sr, ^{96}Nb, ^{96}Tc, ^{105}Rh, ^{141}Ce, and ^{147}Nd had to be resolved from interfering activities by decay. Cesium-134, ^{137}Cs, and ^{85}Sr were determined by gamma-counting radiochemically separated samples, while ^{89}Sr and ^{90}Sr were measured on beta counters which had been calibrated by the method of Bayhurst and Prestwood.[11] Atoms of gamma emitting nuclides were calculated from specific gamma-rays using the gamma branching intensities and half-lives given in the Gamma-Ray Catalog by Reus, Westmier and Warnecke.[12] All nuclides were corrected for decay during the irradiation and for beta or gamma attenuation in the samples.

Experimental Results and Conclusions

Yields for 39 isotopes, either independent (direct formation) or cumulative (produced by direct formation plus the beta-decay of predecessors) were sought in each of the 10 samples. Fig. 3 shows the axial distribution of four of these products: (a) ^{233}Pa, formed by radiative capture which maximizes near z = 9 cm, (b) ^{95}Nb, the fission product with the highest cumulative yield among those we measured, which maximizes near z = 3 cm, (c) ^{227}Th, a high-mass spallation product produced by the p,p5n reaction, which peaks at about 5 cm, and (d) ^{205}Bi, a low-mass spallation product whose yield decreases monotonically with distance into the target. Although certain details of the fission product mass-yield curves change from the front to the back plane, the main features are quite similar. This point is illustrated by Fig. 4 which shows the ratio of the yields of selected fission products to the cumulative yield of ^{95}Nb as a function of axial position. As might be expected, the largest changes occur in the less probable modes of fission, e.g., for low independent yields such as ^{95}Nb and ^{134}Cs, or for neutron deficient isotopes such as ^{87}Y and $^{119}Te^{m}$.

Figure 5a shows the fission product yield-curve from the front-face-foil of the central rod. This mass-yield curve is two-peaked and exhibits several signs of high-energy fission: (a) the shape of the mass-yield curve defined by the cumulative yields (open circles) is quite asymmetric with the heavy peak lower and narrower than the light; (b) the independent

* Amersham Corporation solution number R9/270/46.

yields of antimony isotopes near stability in the mass 120-126 region are comparable to the cumulative yield of ^{127}Sb which would comprise the total 127 chain yield at low energies; and (c) several neutron-deficient isotopes (shown by filled points) were readily measured.

Fission product yields from the outer 9 foils at the front face of the target have been calculated by subtracting the center foil from the data for the entire first plane (see Fig. 5b). None of the neutron-deficient products were observed in these foils. The mass-yield curve appears similar to that from 14-MeV neutron fission of ^{232}Th,[13] which is also shown normalized at mass 99.

Turkevich and Niday proposed that mass yield distributions could be represented by a two-mode-of-fission hypothesis (TMFH)[14] and Ford demonstrated its applicability at intermediate energies.[15] This hypothesis, which suggests that any fission yield curve can be expressed as the combination of symmetric and asymmetric components, has been applied to this data to aid in understanding the curves and to determine the number of fissions. Fourteen-MeV neutron fission of thorium was chosen for the asymmetric or "low-energy-fission" mode since it appears to approximate the secondary fission in the first plane; the amount of fission by this mode was determined from the yields of the four heaviest masses which were measured, ^{140}Ba, ^{141}, ^{143}Ce, and ^{147}Nd. The yields remaining after subtracting the low-energy component are shown in Fig. 5c. The points represent average values, from combining the data from all 10 samples. The Gaussian distribution ("symmetric") which was determined by least squares analysis of the data for ^{72}Zn, ^{89}Sr, ^{95}Nb, ^{103}Ru, ^{105}Rh, and ^{112}Pd, centers about mass 108, has a standard deviation of 14 mass units (FWHM = 33), and has been normalized to 200%.

Figure 5d shows the axial distributions for "symmetric" and "asymmetric" fission and their sum. For the central rod at z = 0.0, the ratio is 2.34, the highest we observed. Figure 6 compares the mass yield curve produced by the TMFH with the experimental data for the entire first plane. The "symmetric to asymmetric" ratio is 1.03. The point at mass 97 is probably low because of independent formation of ^{97}Nb, and mass 115 is low by the yield of $^{115}Cd^{m}$, neither of which were measured. Data for masses 127, 132, and 137 are also expected to be low because of the large charge dispersion in this region in high-energy fission. The lowest ratio of "symmetric to asymmetric", 0.633, occurs at z = 13.11 cm, and the agreement between experimental data and TMFH curve is somewhat better (see Fig. 7). The number of fissions in the sample is determined by summing the mass-yield curve (unnormalized) and dividing by two. A mass-yield curve defined by connecting the data points with straight lines for these two planes gave results that were 12% and 8% lower than the TMFH curves, respectively.

The axial distributions of ^{233}Pa, ^{227}Th, ^{205}Bi, ^{95}Nb, and fission were used to determine the total production per proton in the target. The total number for each reaction is:

$$\text{Total}_i = \frac{M}{\ell \cdot p} \int N_i(z)\, dz$$

where M is the mass of the target in grams, ℓ is the target length in cm, p is the number of protons, and N_i is the number of atoms produced per gram of thorium. The integral was evaluated using Simpson's rule and points read from the graphs as illustrated in Figs. 3 and 5d. Some of our experimental results are shown in Table III. The uncertainty on the number of fissions includes the possibility of a somewhat higher number due to insufficient information on the charge distribution and the yield of nuclides near stability.

In Table III, we also show computational results with and without high-energy fission. For no high-energy fission, we used both the ORNL and RAL models; such a comparison tests differences in evaporation schemes. We used the RAL model with two level density parameter (B_o) values to study high-energy fission effects.

When high-energy fission is neglected, we see the following comparisons between measured and calculated quantities: a) both models predict ^{233}U production to better than 6%, b) the calculated fissions are low by a factor of ~3, c) both models significantly underpredict ^{95}Nb (a fission product) formation and overpredict ^{205}Bi and ^{277}Th production, and d) model predictions intercompare well except for the ^{205}Bi values. When high-energy fission is included, we note the following: a) for B_o = 8 MeV, the calculated ^{233}U production and number of fissions agree very well with measured values, b) for either B_o, the calculated ^{95}Nb and ^{205}Bi production is signficantly improved over the no high-energy fission

case, but there are still marked differences with measured values, and c) for both B_0 values, the calculated ^{227}Th formation is low by a factor of ~2. Based on the comparisons in Table III, we would say that with high-energy fission, the RAL model with B_0 = 8 MeV gives better overall agreement with measurements than with B_0 = 14 MeV (which is the RAL recommended value). This tentative conclusion agrees with that recently reached by the Juelich group.[16]

Further calculated results for the 19-rod clustered thorium target are shown in Table IV. We utilize the $\bar{\nu}$ values to give us an "average" energy for low-energy neutron fission which is then used to predict the low-energy production of the measured fission products. We note for a "frame-of-reference" that the $\bar{\nu}$ values could be attained with a fission mixture of ~70% fission spectrum neutron fission and ~30% 14-MeV neutron fission. Also, the inclusion of high-energy fission adds ~29% to the energy deposition in the target.

A final publication of this thorium conversion measurement is being readied, and will include the effects of a mass-dependent B_0 in the computations as well as measured versus calculated results for more of our experimental data.

Acknowledgements

This work was performed under the auspices of the U.S. Department of Energy. We appreciate the support of E. R. Whitaker, J. R. Baldonado, and K. J. Hughes in setting up the experiment, and the assistance of the counting room personnel in the Los Alamos Nuclear and Radiochemistry group. Many thanks to Antoinette Sandmeier for her typing help.

References

1. G. J. Russell, "Applied Spallation Physics Research at Los Alamos," ICANS-VII, International Collaboration on Advanced Neutron Sources, Chalk River Nuclear Laboratories, Chalk River, Canada, Sept. 12-16, 1983.

2. G. J. Russell, J. S. Gilmore, R. E. Prael, H. Robinson, and S. D. Howe, "Spallation Target-Moderator-Reflector Studies at the Weapons Neutron Research Facility," Symp. on Neutron Cross Sections from 10-50 MeV, Brookhaven National Laboratory, Upton, NY, May 12-14, 1980, BNL-NCS-51245, Vol. I, pp. 169-192 (July 1980).

3. G. J. Russell, J. S. Gilmore, H. Robinson, and R.E. Prael, "Fertile-to-Fissile and Fission Measurements for Depleted Uranium Bombarded by 800-MeV Protons," ICANS-V, Proc. of the 5th Meeting of the International Collaboration on Advanced Neutron Sources, Juelich, West Germany, June 22-26, 1981, Juel-Conf.45, ISSN 0344-5789, pp. 621-639 (Oct. 1981).

4. G. J. Russell, P. W. Lisowski, S. D. Howe, N. S. P. King, and M. M. Meier, "Characteristics of the WNR - a Pulsed Spallation Neutron Source," Nuclear Data for Science and Technology, K. H. Bockhoff, ed., 1983, pp. 831-835.

5. M. S. Livingston, LA-6878-MS, UC-28 and UC-34, Los Alamos National Laboratory (1977).

6. K. C. Chandler and T. W. Armstrong, "Operating Instructions for the High-Energy Nucleon Meson Transport Code HETC," Oak Ridge National Laboratory, Report ORNL-4744 (January 1972).

7. Los Alamos Monte Carlo Group, "MCNP - A General Purpose Monte Carlo Code for Neutron and Photon Transport, Version 2B," LA-7396-M, Revised (April 1981).

8. F. Atchison, "Spallation and Fission in Heavy Metal Nuclei under Medium Energy Proton Bombardment," Meeting on Targets for Neutron Beam Spallation Sources, Juelich, West Germany, June 11-12, 1979, Juel-Conf-34, ISSN 0344-5798, pp. 17-45 (January 1980).

9. R. Gunnink and J. B. Niday, "Computerized Qualitative Analysis by Gamma-Ray Spectrometry," University of California, NTIS, USAEC report UCRL-51061 (1972).

10. J. B. Cummings, "Applications of Computers to Nuclear and Radiochemistry," National Academy of Sciences National Research Council Report NAS-NS-3107, pp, 25-33 (1962).

11. B. P. Bayhurst and R. J. Prestwood, "A Method for Estimating Beta-Counting Efficiences," Nucleonics, 17, No. 3, pp. 82-85 (1959).

12. U. Reus, W. Westmier and I. Warnecke, "Gamma-Ray Catalog," Gesellschaft fuer Schwerionenforschung, Darmstadt, GSI-Report 79-2 (1979).

13. T. R. England, "Preliminary ENDF/B-VI Yields," private communication.

14. A. Turkevich and J. B. Niday, "Fission of ^{232}Th with Pile Neutrons," Phys. Rev. 84, pg. 52 (1951).

15. G. P. Ford, "Analysis of the Two-Mode-of-Fission Hypothesis," Phys. Rev. 118, pg. 1261 (1960).

16. T. W. Armstrong, P. Cloth, D. Filges, and R. D. Neef, "An Investigation of Fission Models for High-Energy Radiation Transport Calculations," Juel-1859, ISSN. 0366-0885 (July 1983).

TABLE I

Physical Characteristics
of the 19-Rod Clustered Thorium Target

Density (g/cm^3)	Diameter (cm)	Length (cm)
11.38	18.28[a]	36.31

[a] Effective diameter ($D = d\sqrt{n}$) for the 19-rod clustered target with an individual rod diameter of 4.194 cm.

TABLE II

Al Monitor Foil Data

Reaction	Cross-Section (mb)		Measured Number of Protons	Statistical Error (%)
$^{27}Al(p,x)^{7}Be$	5.7		1.89×10^{16}	±1.4
$^{27}Al(p,x)^{22}Na$	13.6		1.91×10^{16}	±1.1
$^{27}Al(p,3pn)^{24}Na$	10.8		1.93×10^{16}	±1.3
		Average	1.91×10^{16}	±0.7

TABLE III

Preliminary Experimental Data Compared to Calculated Results
for the Thorium Conversion Measurement

	Experiment	Calculation			
		Without High-Energy Fission		With High-Energy Fission	
		ORNL B_0 = 8 MeV	RAL B_0 = 8 MeV	RAL B_0 = 8 MeV	RAL B_0 = 14 MeV
^{233}U Production (atm/p)	1.25 ± 0.06	1.321 ± 0.009	1.248 ± 0.008	1.267 ± 0.007	1.120 ± 0.007
No. of Fissions (fiss/p)	1.56 ± 0.25	0.550 ± 0.004	0.486 ± 0.004	1.543 ± 0.006	1.444 ± 0.006
^{95}Nb Production (atm/p)	0.068 ± 0.003	0.0300 ± 0.0005	0.0265 ± 0.0005	0.0551 ± 0.0009	0.0523 ± 0.0009
^{205}Bi Production(atm/p)	0.0056 ± 0.0003	0.0500 ± 0.0011	0.0362 ± 0.0010	0.0077 ± 0.0004	0.0080 ± 0.0004
^{227}Th Production(atm/p)	0.046 ± 0.002	0.0644 ± 0.0016	0.0658 ± 0.0016	0.0221 ± 0.0007	0.0236 + 0.0007

TABLE IV

Calculated Thorium Target Characteristics

	Without High-Energy Fission		With High Energy Fission	
	ORNL B_0 = 8 MeV	RAL B_0 = 8 MeV	RAL B_0 = 8 MeV	RAL B_0 = 14 MeV
Protons				
Leakage > 20 MeV (p/p)	0.226 ± 0.003	0.231 ± 0.003	0.228 ± 0.002	0.229 ± 0.002
$\overline{E}$ (Mev)	234.7 ± 4.4	235.6 ± 4.4	239.0 ± 3.2	237.9 ± 3.2
Neutrons				
Leakage > 20 MeV (n/p)	1.019 ± 0.007	1.013 ± 0.006	1.012 ± 0.005	1.040 ± 0.005
$\overline{E}$ (MeV)	93.15 ± 0.97	92.84 ± 0.97	93.12 ± 0.68	90.93 ± 0.67
Leakage < 20 MeV (n/p)	21.01 ± 0.11	19.45 ± 0.11	20.79 ± 0.09	18.82 ± 0.09
$\overline{E}$ (MeV)	---	---	---	2.093 ± 0.017
Capture < 20 MeV (cap/p)	1.321 ± 0.009	1.248 ± 0.008	1.267 ± 0.007	1.120 ± 0.007
$\bar{\nu}$ for Neutron Fission < 20 MeV (n/fiss)	2.773 ± 0.029	2.754 ± 0.029	2.761 ± 0.025	2.840 ± 0.027
$\bar{\varphi}$ < 20 MeV (n/cm^2.s)[a]	---	---	---	$(2.00 \pm 0.01) \times 10^{13}$
Fissions				
High-Energy > 20 MeV (fiss/p)	---	---	0.986 ± 0.005	0.884 ± 0.004
Low-Energy Neutrons < 20 MeV (fiss/p)	0.550 ± 0.004	0.486 ± 0.004	0.557 ± 0.004	0.560 ± 0.004
Energy Deposition				
E > 20 MeV (MeV/p)	421.2 ± 0.8	447.2 ± 0.9	588.2 ± 0.6	583.4 ± 0.6
E < 20 MeV (MeV/p)	122.3 ± 0.8	109.1 ± 0.7	123.9 ± 0.6	122.5 ± 0.6

[a] Average neutron flux inside target for 100 μA of 800-MeV incident protons

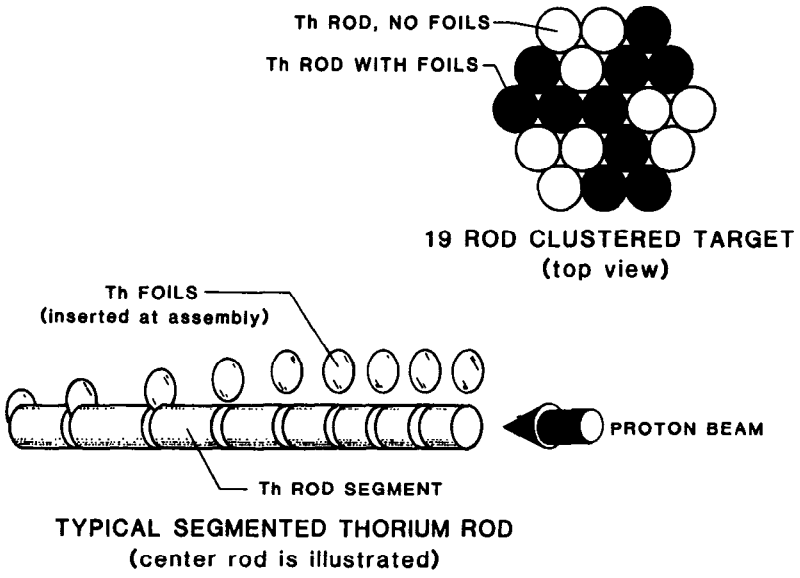

Fig. 1 Illustration of the 19-rod clustered thorium target, the location of the foils in the array, and the foil positions within a rod.

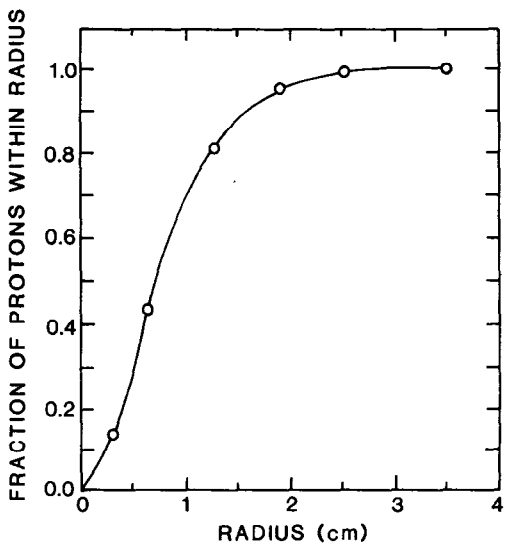

Fig. 2 Measured proton beam profile.

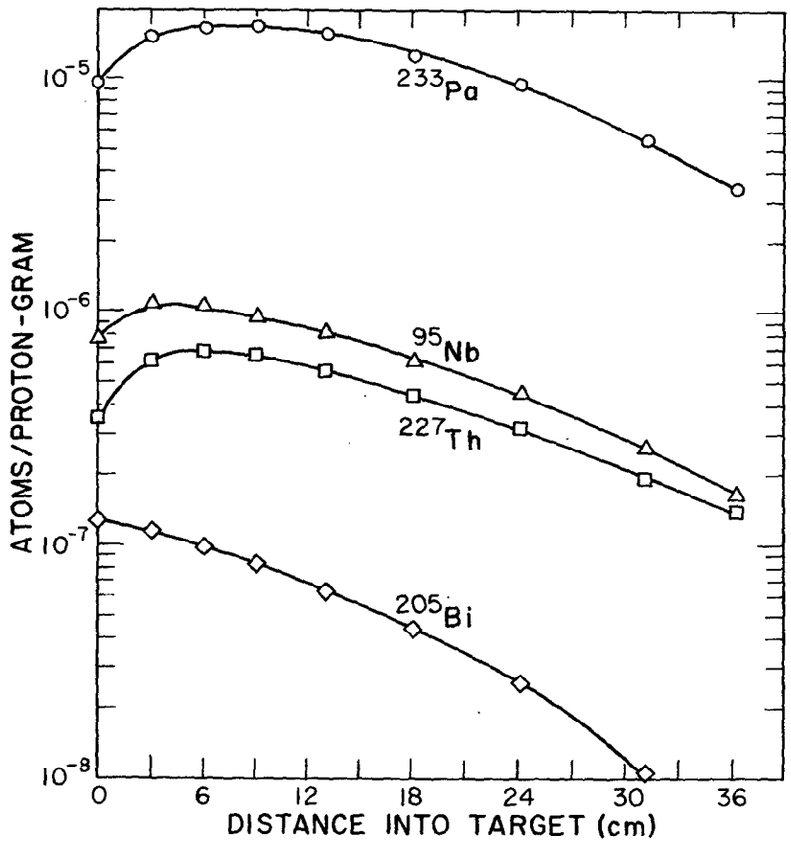

Fig. 3 Axial distributions of ^{233}Pa, ^{95}Nb, ^{205}Bi, and ^{227}Th in the thorium target.

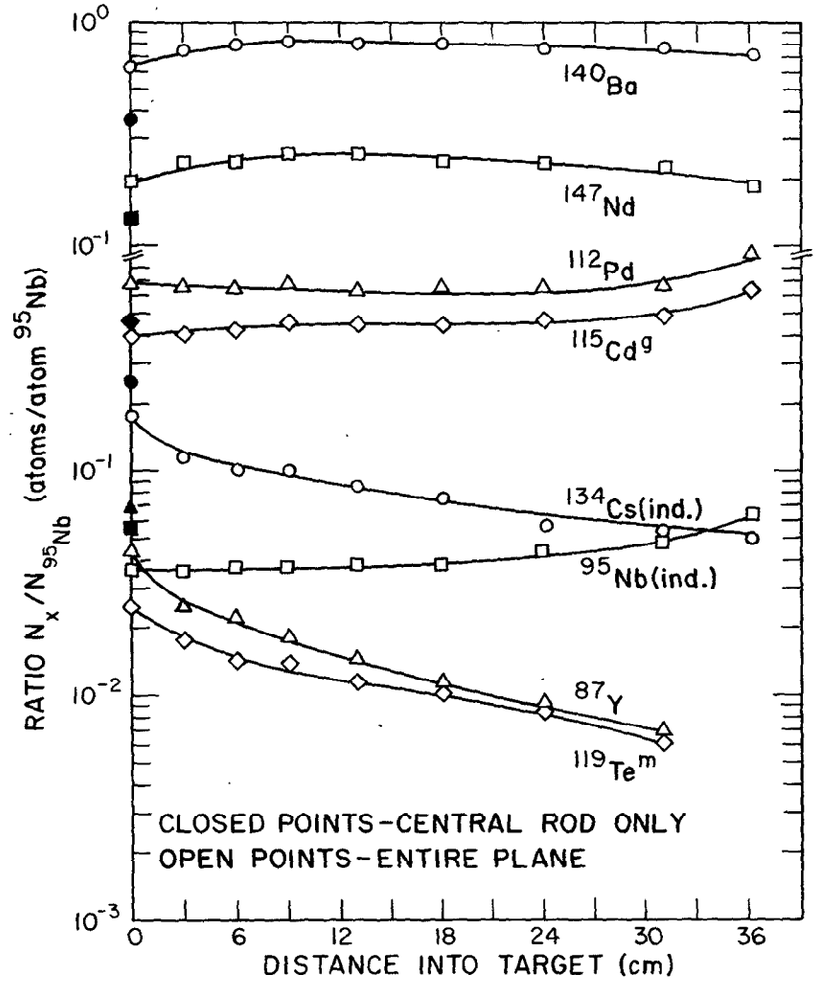

Fig. 4 Ratio of the yields of selected fission products to the cumulative yield of ^{95}Nb as a function of axial position in the thorium target.

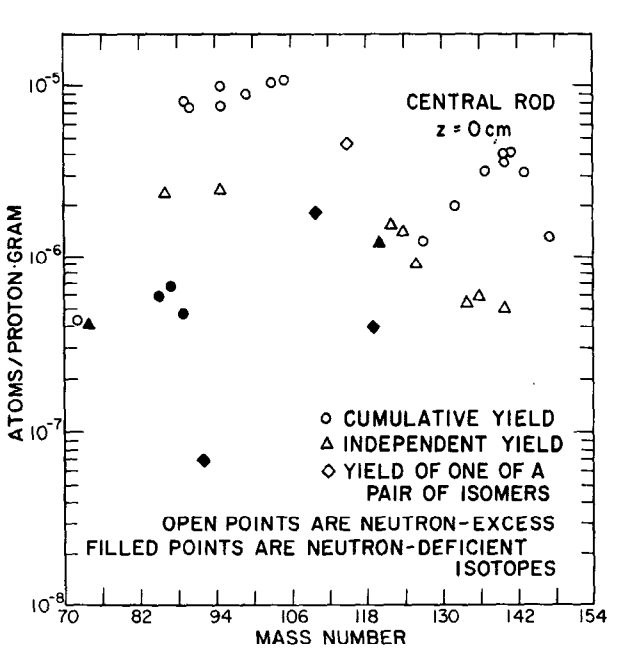

(a)

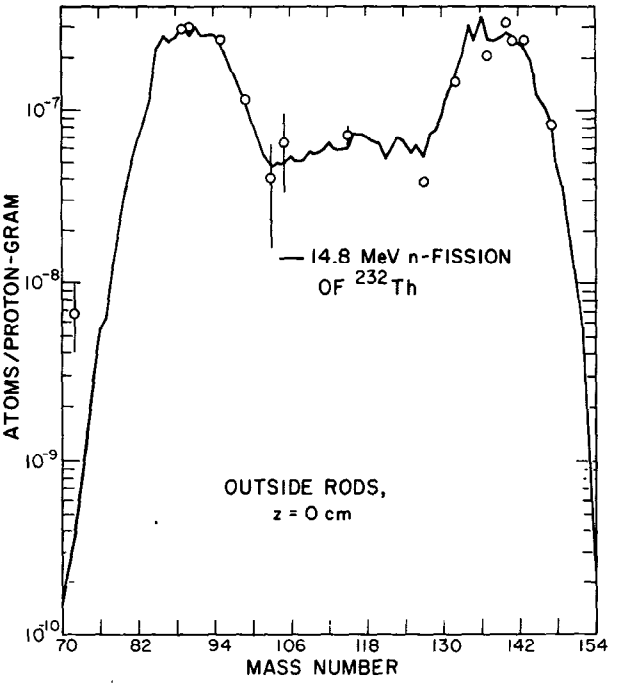

(b)

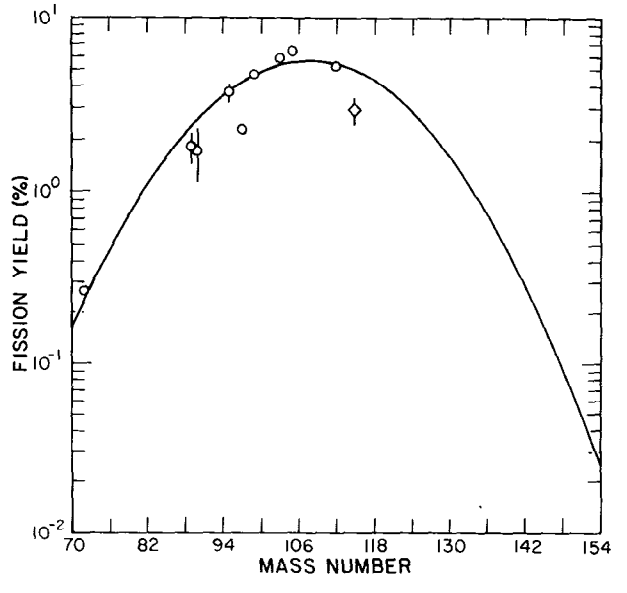

(c)

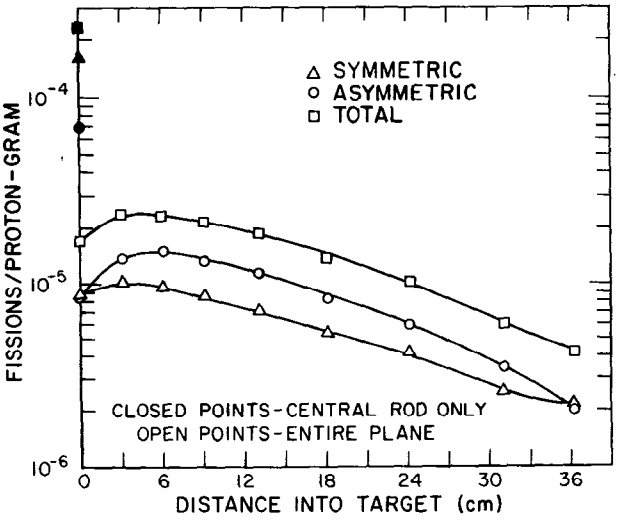

(d)

Fig. 5 Fission data from the thorium target: (a) fission product yields from the central rod, z = 0.0 cm, (b) comparison of the fission product yields from the outside rods, z = 0.0 cm, with yields from 14.7-MeV neutron- fission of ^{232}Th, (c) normalized mass-yield curve for hypothetical "symmetrical" fission mode, and (d) axial distribution of fissions, and of hypothetical "symmetrical" and "asymmetrical" fission modes in the thorium target.

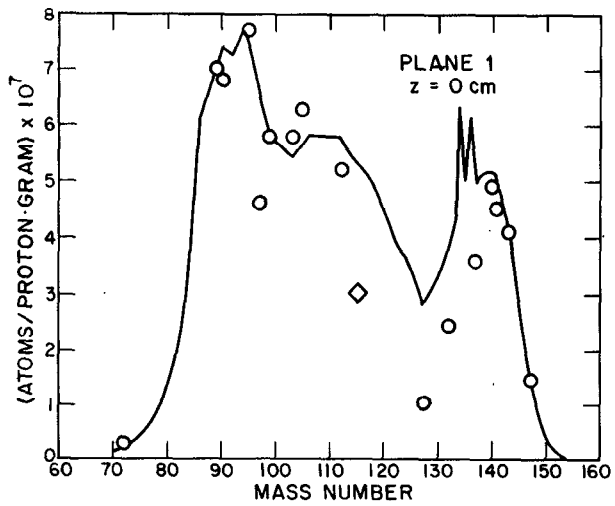

Fig. 6 Comparison of the TMFH mass-yield curve with experimental data from the z = 0.0 cm plane of the thorium target.

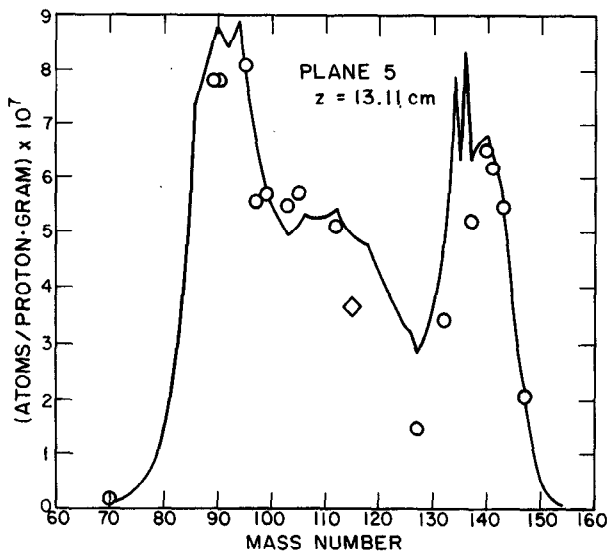

Fig. 7 Comparison of the TMFH mass-yield curve with experimental data from the z= 13.11 cm plane of the thorium target.